Hindawi
Mathematical Problems in Engineering
Volume 2019, Article ID 4014761, 10 pages
https://doi.org/10.1155/2019/4014761

Research Article

Stability Analysis of Underground Multicavities in Bench Blasting Vibration

Deqing Gan, Xi Yang, Yunpeng Zhang, and Xinyu Wei

North China University of Science and Technology, Hebei Mining Key Laboratory of Development and Safety Technology, Tangshan, Hebei 063000, China

Correspondence should be addressed to Xi Yang; ncst-lzy@ncst.edu.cn

Received 15 October 2018; Revised 12 December 2018; Accepted 18 December 2018; Published 2 January 2019

Academic Editor: Mijia Yang

Underground cavities formed by underground mining activities are a potential threat to open-pit mining activities. Longtan Village Iron Mine is located in Chengde city, Hebei province, China. The open-pit mining and underground mining of Longtan Village Iron Mine are simultaneously performed. Cavities will remain after underground mining. When mining is performed on the top of the underground cavities in the open pit, concerns arise regarding the closest distance to prevent the collapse of the cavities. (The closest distance is the safe distance between the explosive and the cavities. If the distance between the explosive and the cavities is less than the closest distance, the stability of the cavities will be affected.) The collapse will endanger the safety of the workers and equipment in the open pit. Therefore, it is necessary to estimate the stability of the underground cavities near the bench blasting. In this paper, a series of bench blast tests was performed, and the site-specific attenuation relations of the *PPV* (Peak particle velocity) and principal frequency of Longtan Village Iron Mine were obtained. Then, an ANASYS three-dimensional numerical model was created, and the propagation of the blast wave and the response of the multicavities were calculated by LS-DYNA. The accuracy of the simulation was verified. However, the bench blast tests do not affect the stability of the cavities. The formula to calculate the closest distance was obtained, which can be used as an approximate guide when designing the bench explosion of Longtan Village Iron Mine. Workers can mine in a safe area of the open pit, and the stability of the cavities will not be affected.

1. Introduction

Underground cavities formed by underground mining activities are a potential threat to open-pit mining activities. When blasting operations are performed on the open-pit steps, the instability of the underground cavities caused by the blasting dynamic disturbances will endanger the safety of workers and equipment in the open pit and will affect the open-pit mining operations. Therefore, it is very important to predict the peak particle velocity that induces instability in an underground cavity.

Dynamic photoelastic experiments were used to simulate the characteristics of a dynamic response of the surrounding rock under tunnel blasting with a small distance by Liu Hui [1], and the field monitoring and numerical simulation of the excavation of Zhaobaoshan tunnel were performed. Then, the blasting excavation methods and safe peak particle velocity were obtained. The peak stress distribution and peak particle velocity distribution of existing tunnels were analysed. Based on the field monitoring of the frequency, amplitude, duration, etc., for deep-hole blasting, the change pattern of the parameters in the propagation process of blast waves in rock masses and the empirical formula of acceleration amplitude were proposed by Long Yuan [2]. Zheng Yingren and Wang Yongfu explored the stability and damage pattern of joint tunnels using the method of indoor similarity model test and numerical analysis, and they quantitatively analysed the stability of joint rock tunnels with the finite element strength reduction method [3]. Xia Xiang determined the attenuation pattern of the peak particle velocity and the principle frequency by field monitoring [4].

In fact, some empirical criteria used to assess the stability of underground cavities are primarily based on the peak particle velocity (*PPV*) of blast waves. For example, based on

the field experiments, some experts proposed key *PPV* values for four damage levels on a cavity rock wall: no damage, slight damage, intermediate damage, and severe damage. When intermediate damage occurs on the cavity rock wall, rock falling will occur in the cavity, and there is a danger of collapse. Under normal circumstances, when the *PPV* of hard rock reaches 0.82-1.11 m/s and the *PPV* of soft rock reaches 0.9-1.07 m/s, there is a risk of collapse in the cavity [5]. Large-scale explosion tests were conducted by U.S. Army engineers between 1948 and 1952. The results of the study showed that the damaged areas of unlined tunnels near sandstone could be divided into four types: intermittent damage, local damage, general damage, and tight closure. The rock in tunnels did not fail until the *PPV* exceeded 0.9 m/s, and intermittent damage would occur in the tunnel when the *PPV* was larger than 0.46m/s [6]. In Persson's Swedish hard rock *PPV* damage criteria, the damage was classified into five levels: initial swelling, initial damage, fragmentation, good fragmentation, and crushing. The threshold damage of the cavity wall occurs if the *PPV* exceeds 1 m/s [7]. Similarly, after conducting a series of tests on the top and bottom of coal mines, Jensen et al. found that no significant damage was found on the rock wall at a *PPV* of 0.445 m/s [8]. Langefors and Kihlstrom studied the stability of granite under blasting vibration. They proposed the *PPV* criteria for blasting vibrations in granite tunnels: a *PPV* of 0.305 m/s results in fall of rock in unlined tunnels; a *PPV* of 0.61 m/s results in new cracks in the rock [9]. Tunstall found that there was no damage in the very-good-quality rocks ($RMR = 85$) when the *PPV* was 0.175 m/s. However, poor-quality rocks (RMR = 49), which were affected by the previous blasting vibrations, sustained minor visible damage when the *PPV* reached 0.046 m/s and serious injuries when the *PPV* reached 0.379 m/s [10]. Calder and Bauer suggested the following relationships: for the *PPV* of 0.254 m/s, no fracturing of intact rock would occur; for the *PPV* of 0.254-0.635 m/s, minor tensile slabbing would occur; for the *PPV* of 0.635-2.54 m/s, strong tensile and some radical cracking would occur; for the *PPV* above 2.54 m/s, complete break-up of the rock mass would occur [11]. Sakurai and Kitamura detected the blasting vibration of the roof and the two gangs of the tunnel. They found that the rock wall would be damaged when the *PPV* was 0.35 m/s, and the rock wall would suffer initial damage when the *PPV* was 0.338 m/s [12]. Dowding classified the tunnel damage into four levels: loosening damage, intermittent damage, local damage, and complete damage. When the *PPV* was 2 m/s, intermittent damage would occur in the tunnel [13]. Oriard found that the underground coal mine rock wall partially loosened when the *PPV* was 0.125-0.38 m/s [14]. The significant variations of these reviewed criteria, which depend on specific site conditions, differ from one another. They cannot be applied as general standards.

Nonetheless, many empirical formulas of *PPV* can be used to estimate the *PPV* for safety assessment of underground cavities. Most *PPV* empirical formulas contain $Q^{1/3}/R$ or $Q^{1/2}/R$, where R is the distance from the blast hole to the point of monitoring and Q is the equivalent TNT charge weight. $Q^{1/2}/R$ is used for the *PPV* prediction of surface blasting, and $Q^{1/3}/R$ is used for the *PPV* prediction of free-field explosion. By using an appropriate attenuation relationship, one can easily obtain the *PPV* that corresponds to a charge weight at a given distance. However, the prediction of the *PPV* is different for different geological media, and there are fewer applications of the *PPV* empirical formula to underground cavities. The geological medium in the underground cavity is discontinuous, and the propagation characteristics of the blast wave also differ from those in the continuous medium. If the safety of the underground cavity must be estimated, the *PPV* inside the cavity must be measured to establish the *PPV* empirical formula that is applicable to the underground cavity. However, it is very dangerous to measure the *PPV* inside the underground cavity. In this paper, a combination of field experiment and numerical simulation is proposed to calculate the *PPV* to estimate the safety of underground cavities.

In addition to the amplitude and geotechnical conditions of the blast wave, the structural response also depends on the vibration frequency of the blast wave. The principle frequency (*PF*) of blast waves is particularly important. At present, there are not many empirical formulas for *PF* attenuation [15–17]. Some experts conducted numerical simulation studies and obtained the *PF* attenuation law of blast waves propagated in granite [18]. Based on a large number of observation experiments, some empirical *PF* attenuation relations have been proposed [19–24]. However, like the *PPV*, the field dependency of the *PF* is also strong. The *PF* empirical formula must be obtained according to the actual situation of the experimental site.

In this paper, the stability of multicavities below the open pit under the influence of blasting vibration is analysed. Some small-scale blasting vibration tests were performed in the open pit. Field blasting test data were measured to obtain the site-specific empirical formula of the *PPV* and *PF* of blast waves. Then, an ANASYS numerical model was established. Based on the *PPV* empirical formula and PF empirical formula, blast waves at different locations were applied to the model, and the blast wave propagation and cavity response were calculated by LS-DYNA. The measured data were used to verify the accuracy of the numerical simulations. Very good consistency between the measured and numerically simulated data was obtained. Finally, according to the numerically simulated data of the cavities, the stability of the cavities under blasting vibration was analysed, and the closest distances of the different charge weights were obtained.

2. Site Description

The site under consideration, Longtan Village Iron Mine, is situated near the town of Longtan, approximately 50 km northwest of Chengde city in north China. Five levels are mined in the mine: they are 950 m, 940 m, 920 m, 913 m, and 890 m levels. The mining method was the open stope method. The cavities have not been dealt with, and a small number of cavities were found to fall. Thus, underground mining is increasingly dangerous, and the mine has been turned

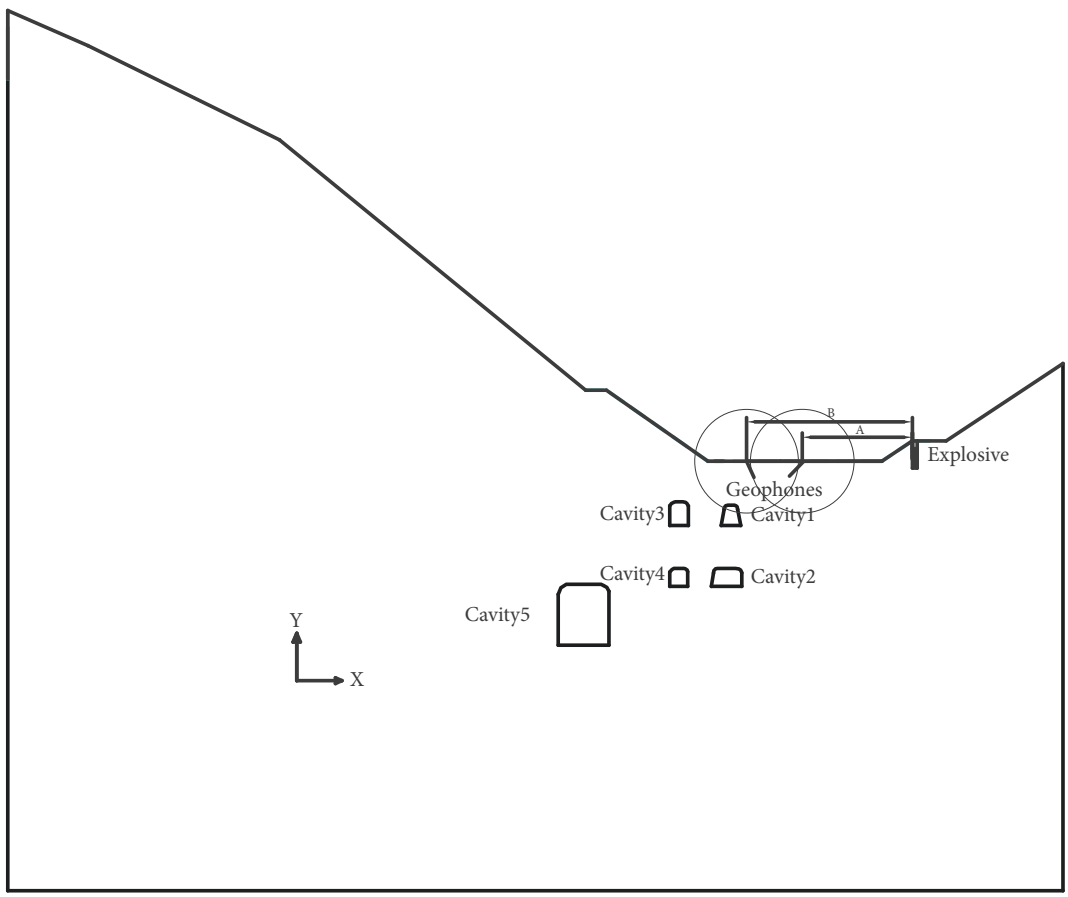

Figure 1: Test site profile.

into open-pit mining. Many cavities below the open pit have collapsed in different degrees because of the influence of the ground pressure, rock weathering, and blasting vibration. In the open-pit mining process, these cavities with complex shapes and different heights seriously threaten the safety of the people and equipment in the open pit. Therefore, the stability of the cavities must be analysed before large-scale mining in the open pit.

3. Experimental Design and Setup

Some small-scale blast tests were performed at locations with more cavities. The relevant information is shown in Figure 1. The step height is 7 m, the slope angle is approximately 40°, and the overburden thickness of the cavity is 13.3 m. A and B indicate the distance between the two blast vibration monitors to the explosion zone. The relevant mechanical parameters of the rock were measured before the blast tests and are shown in Table 1.

4. Test Results

In total, four tests were conducted. The data are shown in Table 2. Figure 2 shows the velocity time histories of test No. 2 with a charge weight of 400 kg recorded at 29 m from the bench blast hole. Figure 3 shows the velocity time histories of test No. 2 with a charge weight of 400 kg recorded at 37 m from the bench blast hole. When the distance is A, the vibration velocity in the x direction dominates. However, the proportion of vibration velocity in the three directions is gradually uniform with the increase in distance.

The vibration frequency of the blast wave also plays a crucial role in the dynamic response of the rock mass. With the same charge weight, the frequency band of the blast wave always narrows when the distance increases, and the value decreases because high-frequency energy attenuates faster than low-frequency energy. The principle frequency of the blast wave must be analysed.

The fitting formula of the peak particle velocity and the principle frequency in the three directions of x, y, and z are as follows.

X direction:

$$PPV = 1.2543\left(\frac{\sqrt[3]{Q}}{R}\right)^{1.2280} m/s \quad \left(r^2 = 0.9759\right) \tag{1}$$

$$PF = 132.2209\left(\frac{\sqrt[3]{Q}}{R}\right)^{1.2749} Hz \quad \left(r^2 = 0.9451\right) \tag{2}$$

Table 1: Rock mechanics parameters.

ρ(kg/m^3)	E(GPa)	μ	Compressive strength(MPa)	c (MPa)	Φ (°)
2700	40.31	0.22	129.45	2.29	36

Table 2: Summary of four bench blast tests.

Test number	Actual charge mass (kg)	Distance (m)	Point number	*PPV* (m/s)			Resultant velocity (m/s)	*PF* (Hz)		
				X	Z	Y		X	Z	Y
1	380	37(A)	1	0.16	0.11	0.12	0.16	17	20	22
	380	80(B)	2	0.06	0.03	0.03	0.05	5	4	7
2	400	29(A)	1	0.25	0.14	0.17	0.26	23	19	30
	400	37(B)	2	0.17	0.11	0.11	0.17	17	17	24
3	420	38(A)	1	0.18	0.13	0.07	0.20	18	13	17
	420	80(B)	2	0.07	0.04	0.04	0.06	7	6	8
4	460	45(A)	1	0.13	0.09	0.11	0.15	12	13	16
	460	80(B)	2	0.08	0.05	0.05	0.08	8	6	9

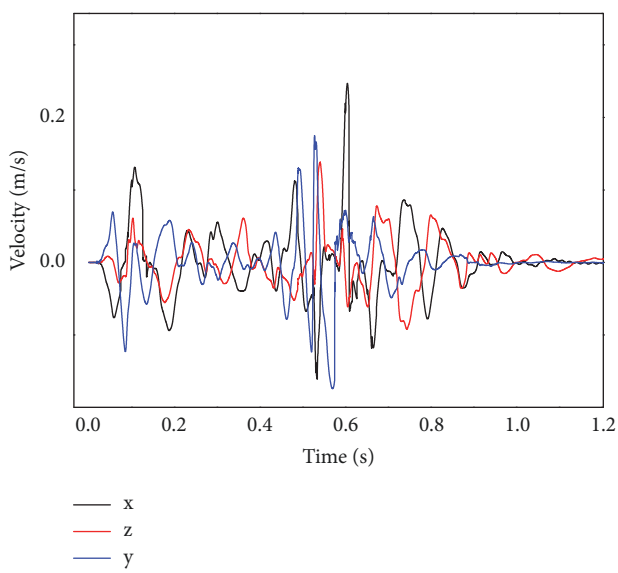

Figure 2: Velocity time histories of test No. 3 recorded at 29 m from the bench blasting hole.

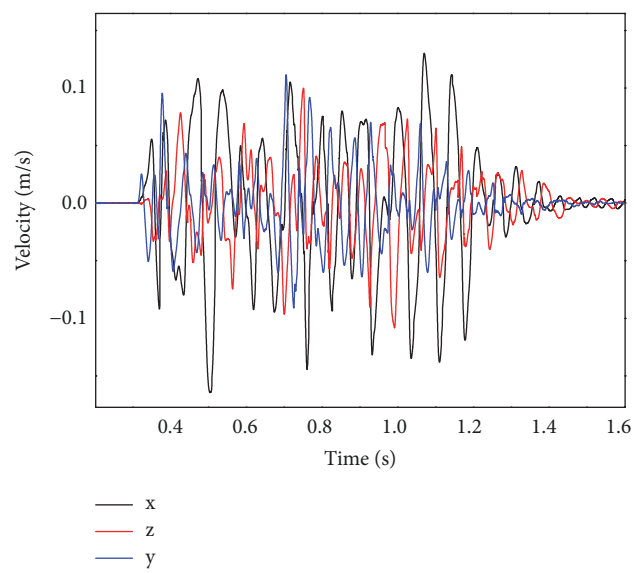

Figure 3: Velocity time histories of test No. 3 recorded at 37 m from the bench blasting hole.

Z direction:

$$PPV = 0.6875\left(\frac{\sqrt[3]{Q}}{R}\right)^{1.2125} m/s \quad \left(r^2 = 0.9431\right) \tag{3}$$

$$PF = 157.5071\left(\frac{\sqrt[3]{Q}}{R}\right)^{1.4296} Hz \quad \left(r^2 = 0.9207\right) \tag{4}$$

Y direction:

$$PPV = 0.8013\left(\frac{\sqrt[3]{Q}}{R}\right)^{1.2786} m/s \quad \left(r^2 = 0.8384\right) \tag{5}$$

$$PF = 171.3957\left(\frac{\sqrt[3]{Q}}{R}\right)^{1.3006} Hz \quad \left(r^2 = 0.9600\right) \tag{6}$$

R is the distance from the blast hole to the point of monitoring (m). Q is the equivalent TNT charge weight (kg). PF is the principle frequency of the blast wave (Hz). PPV is the peak particle velocity (m/s).

5. Numerical Model and Calibration

The cavities with poor stability are selected to establish a three-dimensional model as shown in Figure 5. There is no large-scale stratification in the study area after the geological survey. The rock integrity is better than others. Thus, it is assumed that the model material is continuous and homogeneous in the simulation process. The specific mechanical parameters of material are shown in Table 1. It is difficult to establish a model that contains the entire site. A 1/2 three-dimensional model is established to overcome this problem. The model is 258 m long in the x direction, 260 m and 157 m high in the y direction, and 55 m wide in the z

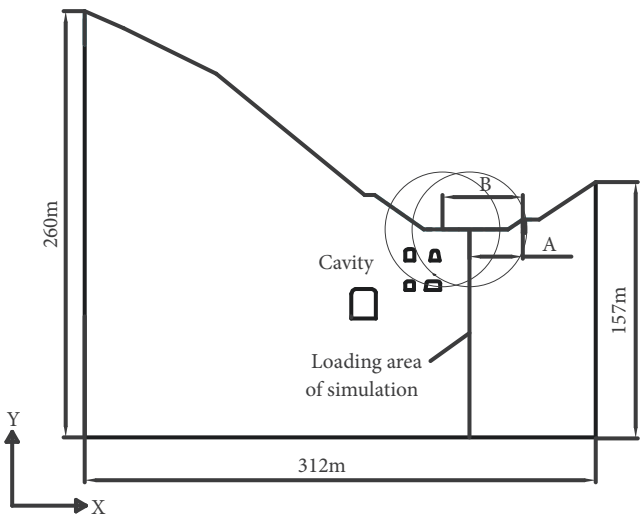

Figure 4: Loading area at the model boundary.

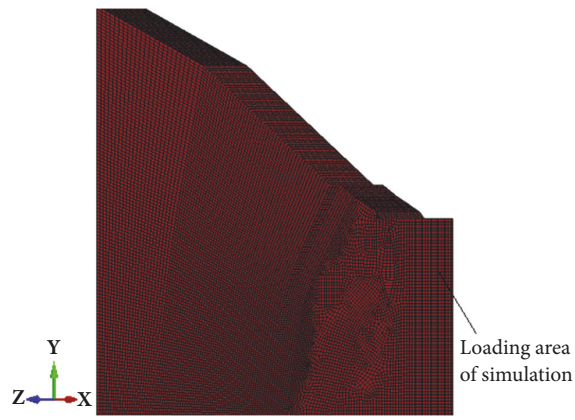

Figure 5: Loading area at the model boundary.

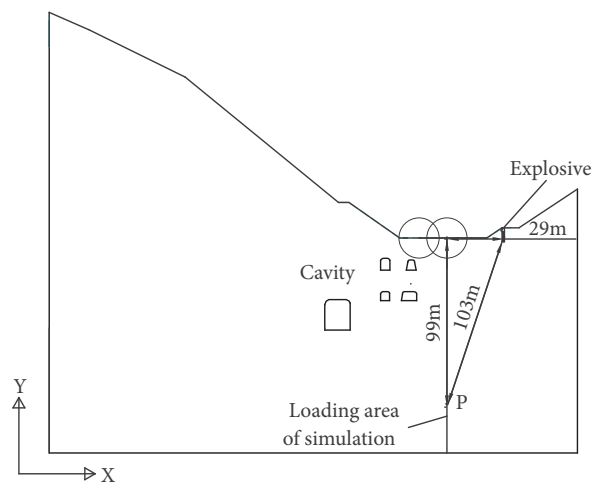

Figure 6: Illustration of the estimation of the velocity time history at point P.

direction. The size of the model is determined by calculating the time required for the blast wave propagation from the cavity to the numerical boundary, which is longer than the duration of the recorded velocity histories in Figure 2. To ensure that the blast wave can effectively propagate to the boundary of the cavity wall and there is enough time for reflection, the simulation time is approximately twice as long as the duration of the recorded velocity time history in Figure 2. The model is surrounded by a transmission boundary, and the top is a free surface. The bottom is a transmission boundary. No blasting model is installed in the model. Instead, the blast wave loading is used. First, the blast wave loading surface is selected as shown in Figure 4. This surface is also a boundary in the three-dimensional model, as shown in Figure 5. Second, the blast waves that must be loaded at different positions on the loading surface are calculated according to the peak particle velocity and principle frequency fitting formula. Finally, the blast wave at different locations in the model can be obtained.

The surface that corresponds to distance A is selected as the loading surface, as shown in Figure 4. The velocity time histories in Figure 2 are selected as the basic data for the calculation of the blast wave at other points on the loading surface. For example, at point P in Figure 6, the distance from the blast hole to point P is 103 m. The *PPV* at point P in three directions can be obtained according to the fitting formula of the *PPV*. Then, the ratio of the *PPV* in the three directions of point P to the *PPV* in the three directions of point A can be obtained. Finally, the velocity time histories in Figure 2 are multiplied by this ratio to obtain the velocity time histories in three directions of point P. Thus, the velocity time histories in three directions at different positions on the loading surface can be obtained. Similarly, the principle frequency in three directions at different locations on the loading surface can also be obtained. The difference is that the principle frequency of point P is achieved by changing the time step of the velocity time histories in Figure 2.

It is also necessary to calculate the arrival time of blast waves at various points on the loading surface after completing the above steps. The P-wave dominates the blast wave in the site as observed. The P-wave velocity of the blast wave is defined by [25]

$$C = \sqrt{\frac{E(1-\mu)}{\rho(1+\mu)(1-2\mu)}} \tag{7}$$

where E is the modulus of elasticity (Pa); μ is Poisson's ratio; ρ is the density (kg/m^3).

After completing the calculation of the blast wave velocity, the initial arrival time of the blast wave loading at different points on the loading surface can be calculated as follows

$$t = \frac{L-29}{C} \tag{8}$$

where L is the distance from different points on the loading surface to the blast hole (m); t is the initial arrival time (s); C is the blast wave velocity (m/s); 29 is distance A (m). The 3D solid element is used in the model. Furthermore, the model is meshed with a mesh size of 2 m. The ∗MAT_PLASTIC_KINEMATIC material model is chosen to

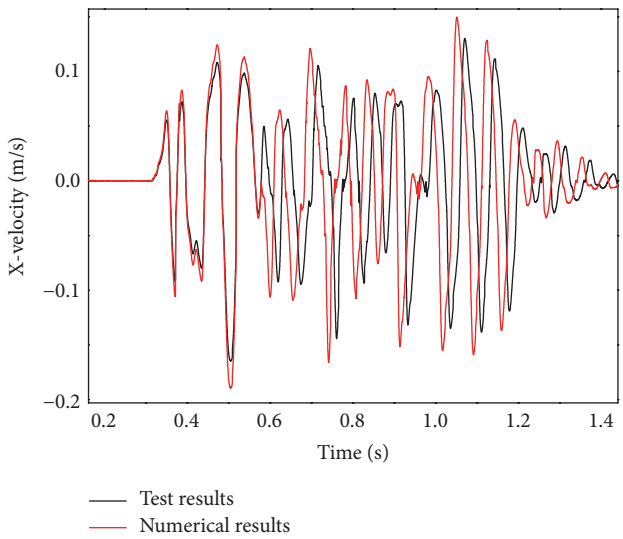

Figure 7: Comparison of the x-velocity time histories from the numerical simulation and field test.

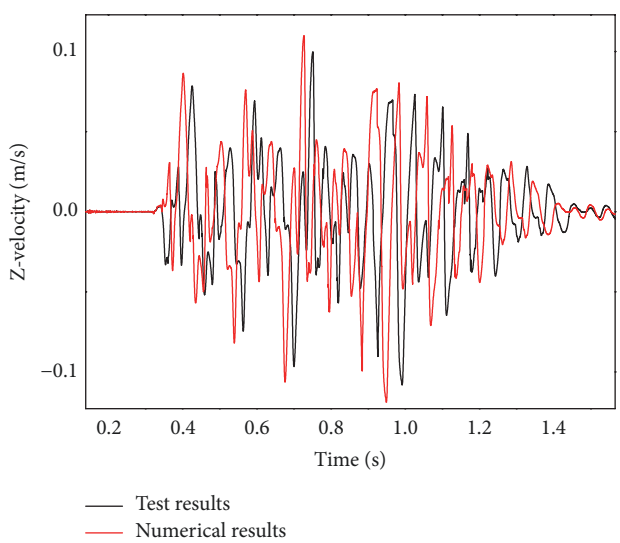

Figure 8: Comparison of the z-velocity time histories from the numerical simulation and field test.

simulate the rock mass behaviour. Finally, the velocity time histories at the point of distance B in the model are compared with those in the field experiment. The results are shown in Figures 7–9. Very good consistency between the measured and numerically simulated data is obtained.

6. *PPV* Damage Criteria

As reviewed above, the *PPV* damage criteria are widely used. However, these damage criteria vary from one another due to the different material properties of the rock and conditions of the test site [26–30]. The criteria developed by Li and Huang in Table 3 were selected because they provided various *PPV* values for different rock masses in terms of the rock mass compressive and tensile strengths, which are more consistent

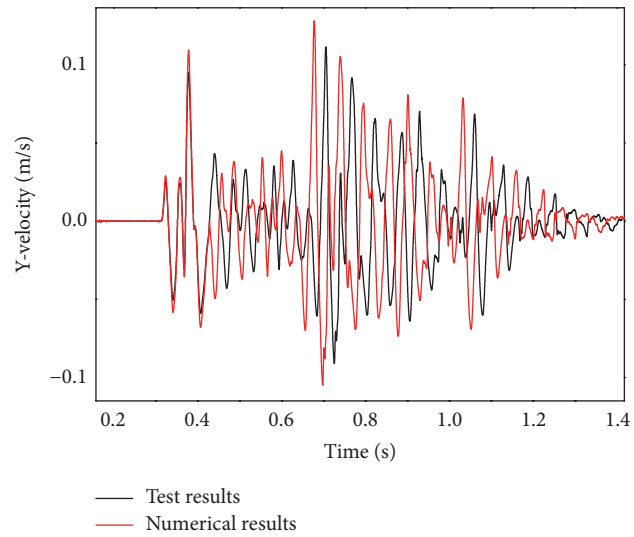

Figure 9: Comparison of the y-velocity time histories from the numerical simulation and field test.

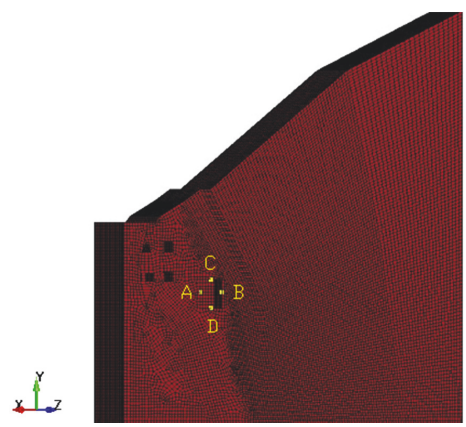

Figure 10: : Location of the recording points.

with the actual situation. Without loss of generality, 0.96 m/s is chosen as the *PPV* damage criterion according to the data in Table 3 and the rock strength of the test site.

7. Numerical Simulation of the Cavity Stability

As shown in Figure 10, measurement points A, B, C, and D are taken from the cavity walls, roof, and floor. The *PPV*s are extracted as shown in Figures 11–13. Point A of each cavity has the largest *PPV*, followed by point C because points A and C face the blasting area, and the distance is short. In addition, point A has a larger *PPV* than point C because of different angles of the incident waves at the two points. The distances between points B and D and the blast hole are long, and the blast waves are blocked by the cavity, so the *PPV*s of points B and D are small. The most dangerous point in the cavity is point A.

The *PPV*s of point A of 5 cavities in three directions are shown in Figure 14. The *PPV* does not exceed 0.96 m/s, so the stability of the cavities will not be affected. In addition, the

Table 3: Critical vibration velocity of the wall rock of the grotto[5].

Compressive strength (MPa)		Tensile strength (MPa)	No damage (m/s)	Slight damage (m/s)	Intermediate damage (m/s)	Serious damage (m/s)
Hard rock	75–110	2.1–3.4	0.27	0.54	0.82	1.53
	110–180	3.4–5.1	0.31	0.62	0.96	1.78
	180–200	5.1–5.7	0.36	0.72	1.11	2.09
Soft rock	40–100	1.1–3.1	0.29	0.58	0.90	1.67
	100–160	3.4–4.5	0.35	0.70	1.07	1.99

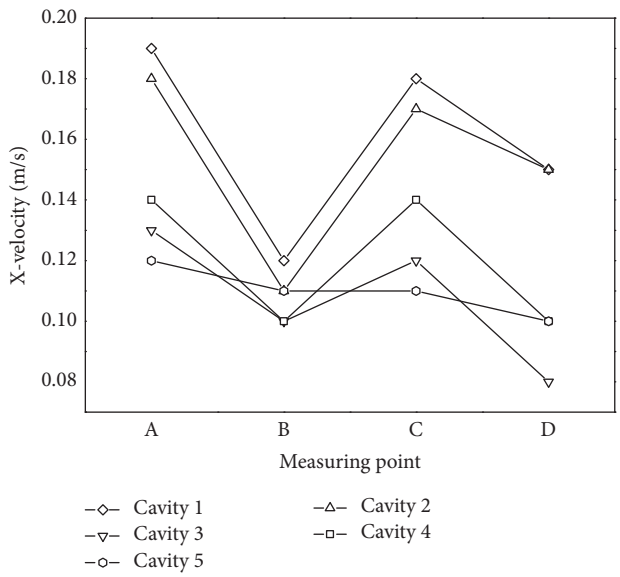

Figure 11: Peak particle velocity of the recording points in the x direction.

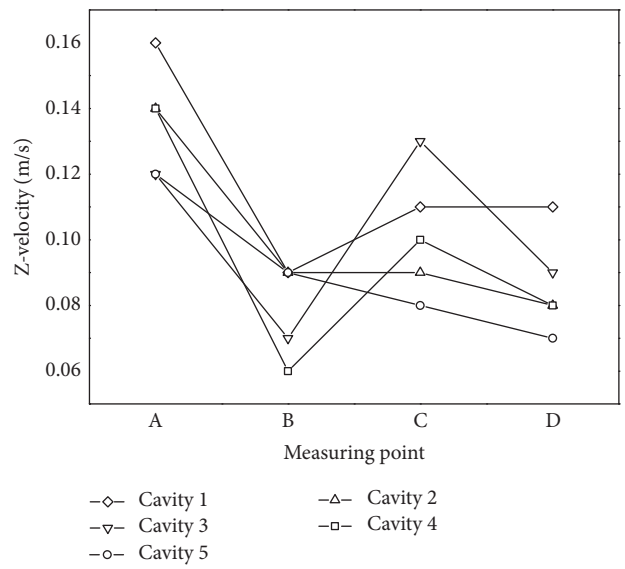

Figure 12: Peak particle velocity of the recording points in the z direction.

PPV in the x direction is the largest and significantly larger than those in the other two directions.

Another measurement point (point E) in Figure 15 was extracted. The distances from the blast hole to points A and E are identical. The *PPV*s of points A and E of the five cavities in the x direction are shown in Figure 16. The *PPV* of point A is larger than the *PPV* of point E because of the reflection of the blast wave on the surface of the cavity wall. Therefore, the fitting formula must be established according to the *PPV* on the cavity wall. The simulation data of point A in the x direction are shown in Table 4.

The following fitting formula is established based on the *PPV* of point A of the five cavities in the x direction.

$$PPV = 1.4129\left(\frac{\sqrt[3]{Q}}{R}\right)^{1.0694} m/s \quad \left(r^2 = 0.9526\right) \tag{9}$$

The *PPV* damage criterion is 0.96 m/s. Combined with formula (9), the closest distance formula applicable to the cavities can be obtained as formula (10). The closest distance that corresponds to a charge weight can be easily obtained according to formula (10). The closest distance is the safe distance between the explosive and the cavities. If the distance between the explosive and the cavities is less than the closest distance, the stability of the cavities will be affected.

Table 5 gives some estimated closest distances at different charge weights. Table 5 and formula (10) can be used as an approximate guide when designing the bench explosion of Longtan Village Iron Mine.

$$R^* = \frac{\sqrt[3]{Q}}{(0.96/1.4129)^{1/1.0694}} m \tag{10}$$

R^* is the closest distance in different charge masses (m). Q is the equivalent TNT charge weight (kg).

The closest distance is the safe distance between the explosive and the cavities. If the distance between the explosive and the cavities is less than the closest distance, the stability of the cavities will be affected.

8. Discussion

It is very dangerous to perform experiments above or inside cavities, so we cannot experimentally obtain formula (9). The experiment can be conducted outside the cavities to obtain formulas (1)-(6). Then, numerical simulation can be conducted. The simulation results outside the cavities are consistent with the experimental results. When the blast wave passes to the cavities, the simulation results in the cavities should also be consistent with the actual situation in the cavities. The loaded blast wave is accurate outside the cavities.

Table 4: Simulation data of point A in the X direction.

Cavity number	Actual charge mass(kg)	Distance (m)	*PPV* of X direction (m/s)
1	400	48	0.19
2	400	51	0.18
3	400	65	0.13
4	400	68	0.14
5	400	73	0.12

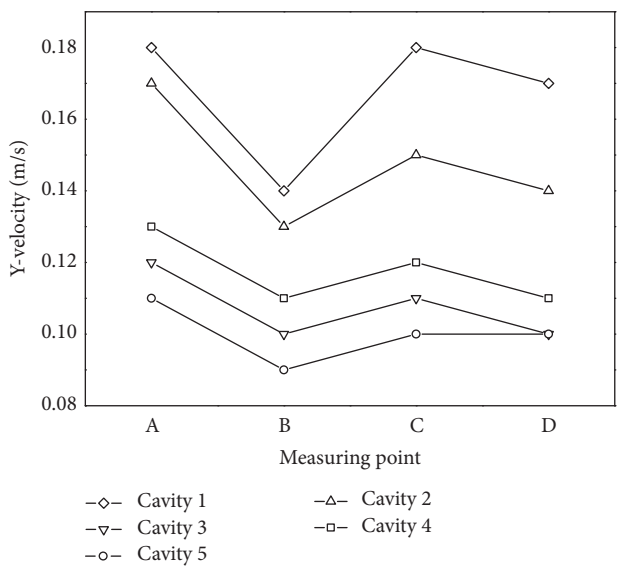

Figure 13: Peak particle velocity of the recording points in the y direction.

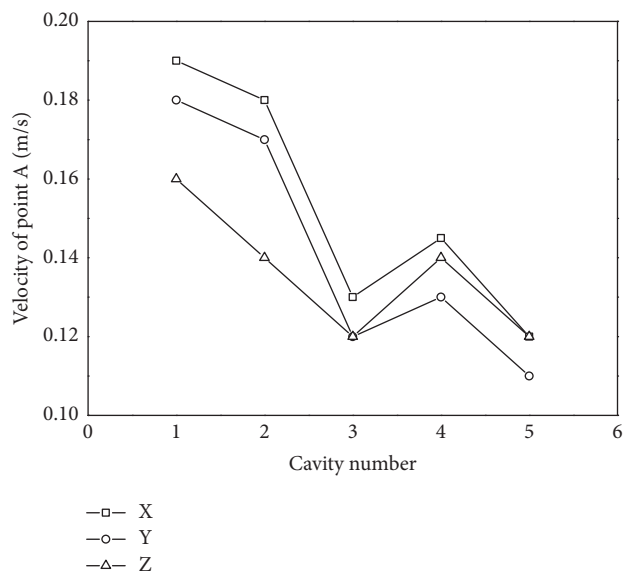

Figure 14: Peak particle velocity of point A of different cavities.

Table 5: Closest distance of different charge weights.

Charge mass (kg)	Closest distance (m)
380	10.40
760	13.10
1140	14.99
1520	16.50
1900	17.78
2280	18.89

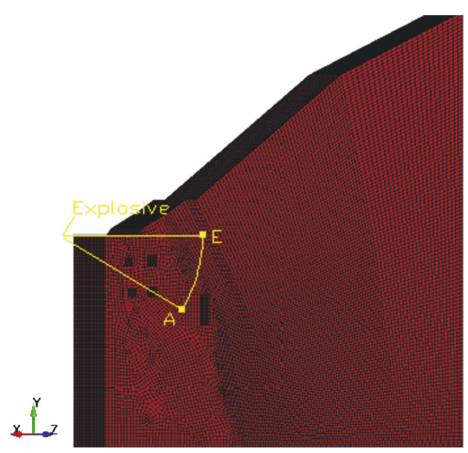

Figure 15: Location of the recording points.

Thus, the PPV inside the cavities should also be accurate. The site-specific attenuation relations of the PPV inside the cavities can be obtained. The stability of underground cavities can be analysed. Formula (1) is different from formula (9). Because the reflection of the blast wave occurs when it is passed to the cavities, as shown in Figure 15, the PPV attenuation relations of point E are identical to those in formula (1) when there is no blast wave reflection.

Although some research results have been obtained in this paper, more accurate simulation results are required. There are many methods to predict the blasting vibration. M. Hasanipanah proposed an imperialistic competitive-algorithm-based fuzzy system to predict mine blasting [31]. Nazanin Fouladgar and Mahdi Hasanipanah used the cuckoo search algorithm to estimate the peak particle velocity in mine blasting [32]. Maryam Amiri, Hassan Bakhshandeh Amnieh, and Mahdi Hasanipanah combined artificial neural network and K-nearest neighbour models to predict the blast-induced ground vibration and air-overpressure [33]. Masoud Monjezi and Mahdi Hasanipanah evaluated the blast-induced ground vibration at Shur River Dam, Iran, using an artificial neural network [34]. Khalil Taheri and Mahdi Hasanipanah proposed a hybrid artificial bee colony

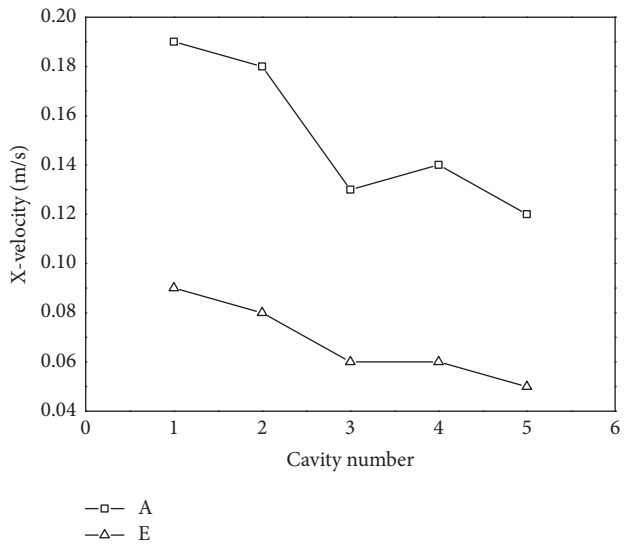

Figure 16: Peak particle velocity of points A and E of different cavities in the x direction.

algorithm-artificial neural network to forecast the blast-produced ground vibration [35, 36]. These methods are very accurate and suitable for predicting the blasting vibration, which we may combine with simulation to obtain more accurate PPV values in the future.

9. Conclusions

A series of bench blast tests was carried out, and the site-specific attenuation relations of the *PPV* and principal frequency of Longtan Village iron ore were obtained. A three-dimensional numerical model was created. The measured data were used to verify the accuracy of the numerical simulations. Very good consistency between the measured and numerically simulated data was obtained, and the bench blast tests did not affect the stability of the cavities. The formula to calculate the closest distance that would not cause damage to the existing cavities was obtained. The closest distances of the charge weights of 380 kg, 760 kg, 1140 kg, 1520 kg, 1900 kg, and 2280 kg are 10.40 m, 13.10 m, 14.99 m, 16.50 m, 17.78 m, and 18.89 m, respectively. The formula can also be used to calculate the closet distance in the case of other charge weights. Those can be used as an approximate guide when designing the bench explosion of Longtan Village Iron Mine.

Although some research results have been obtained, more accurate simulation results are required, which may be obtained in combination with various methods. The geological conditions studied in this paper are relatively simple and require further research in the future.

Data Availability

The blasting data used to support the findings of this study are included within the article.

Conflicts of Interest

The authors declare no conflicts of interest.

Authors' Contributions

Deqing Gan, Xi Yang, and Yunpeng Zhang wrote the main manuscript text and Xinyu Wei prepared all figures.

Acknowledgments

The research is mainly supported by National Natural Science Foundation of China (51374087) and Natural Science Foundation of Hebei Province (E2016209388).

References

[1] H. Liu, "Dynamic responses of hoof-shaped tunnels to adjacent blastings," *Explosion and Shock Waves*, vol. 20, no. 2, pp. 175–181, 2000.

[2] Y. Long, "Study on propagation characteristics of blasting seismic waves in a rock medium and numerical calculation," *Engineering Blasting*, vol. 6, no. 3, pp. 1–7, 2000.

[3] Y. Zheng, Y. Wang, C. Wang et al., "Stability analysis and exploration of failure law of jointed rock tunnel-seminor on tunnel stability analysis," *Chinese Journal of Underground Space and Engineering*, vol. 7, no. 4, pp. 649–656, 2011.

[4] X. Xia and J. Li, "Udec modeling of vibration characteristics of jointed rock mass under explosion," *Rock and Soil Mechanics*, vol. 26, no. 1, pp. 50–56, 2005.

[5] Z. Li and H. Huang, "The calculation of stability of tunnels under the effects of seismic wave of explosions," in *Proceedings of the 26th Department of Defense Explosives Safety Seminar*, US Department of Defense Explosives Safety Board, 1994.

[6] A. J. Hendron, "Engineering of rock blasting on civil projects," in *Structural and Geotechnical Mechanics, A Volume Honoring NM Newmark*, W. J. Hall, Ed., pp. 242–247, Prentice-Hall, Englewood Clis, NJ, USA, 1977.

[7] P.-A. Persson, "Relationship between strain energy, rock damage, fragmentation, and throw in rock blasting," *International Journal of Blasting Fragment*, no. 1, pp. 99–110, 1997.

[8] D. E. Jensen, R. D. Munson, L. L. Oriard et al., "Underground Vibrations from Surface Blasting at Jenny Mine, KY Woodward-Clyde Consultants, Orange CA. Final Contract RPTJ0275030 for US Bureau of Mines," 1979.

[9] U. Langefors and B. Kihlstrom, *The Modern Technique of Rock Blasting*, John Wiley & Sons Inc, California, USA, 3rd edition, 1978.

[10] A. M. Tunstall, "Damage to underground excavations from open-pit blasting," *Trans Inst Min Met (Sect A: Min Ind)*, vol. 106, pp. A19–A24, 1997.

[11] P. N. Calder and A. Bauer, "The Influence and Evaluation of Blasting on Stability. Stability in Open Pit Mining," in *Society of Mining Engineers of the American Institute of Mining, Metallurgical and Petroleum Engineers*, pp. 83–94, NY, USA, 1971.

[12] S. Sakurai and Y. Kitamura, "Vibration of tunnel due to adjacent blasting operation," in *Proceedings of the International Symposium on Field Measurement in Rock Mechanics*, pp. 61–77, Switzerland, Zurich, 1977.

[13] C. H. Dowding, "Estimating earthquake damage from explosion testing of full-scale tunnels," *Adv Tunn Tech Subsurf Use*, vol. 4, no. 3, pp. 113–117, 1984.

[14] L. L. Oriard, "Blasting effects and their control in open-pit mining," in *Geotechnical Practice for Stability in Open-Pit Mining*, C. O. Brawner and V. Milligan, Eds., p. 197, SME/AIME Publication, 1972.

[15] T. N. Singh, R. Kanchan, K. Saigal, and A. K. Verma, "Prediction of P-wave velocity and anisotropic properties of rock using artificial neural networks technique," *Journal of Scientific and Industrial Research*, vol. 63, pp. 32–38, 2004.

[16] D. E. Siskind, M. S. Stagg, J. W. Kopp, and C. H. Dowding, "Structure Response and Damage Produced by Ground Vibration from Surface Blasting," in *Report of Investigations 8507*, DC, US Bureau of Mines, Washington, USA, 1980.

[17] M. T. Mohamed, "Artificial neural network for prediction and control of blasting vibrations in Assiut (Egypt) limestone quarry," *International Journal of Rock Mechanics and Mining Sciences*, vol. 46, no. 2, pp. 426–431, 2009.

[18] C. Wu and H. Hao, "Numerical study of characteristics of underground blast induced surface ground motion and their effect on above-ground structures. Part I. Ground motion characteristics," *Soil Dynamics and Earthquake Engineering*, vol. 25, no. 1, pp. 27–38, 2005.

[19] H. Hao, Y. Wu, G. Ma, and Y. Zhou, "Characteristics of surface ground motions induced by blasts in jointed rock mass," *Soil Dynamics and Earthquake Engineering*, vol. 21, no. 2, pp. 85–98, 2001.

[20] O. Yilmaz and T. Unlu, "Three dimensional numerical rock damage analysis under blasting load," *Tunnelling and Underground Space Technology*, vol. 38, no. 9, pp. 266–278, 2013.

[21] G. Tripathy, R. Shirke, and M. Kudale, "Safety of engineered structures against blast vibrations: A case study," *Journal of Rock Mechanics and Geotechnical Engineering*, vol. 8, no. 2, pp. 248–255, 2016.

[22] M. Cardu and J. Seccatore, "Quantifying the difficulty of tunnelling by drilling and blasting," *Tunnelling and Underground Space Technology*, vol. 60, pp. 178–182, 2016.

[23] B. Mobaraki and M. Vaghefi, "Numerical study of the depth and cross-sectional shape of tunnel under surface explosion," *Tunnelling and Underground Space Technology*, vol. 47, pp. 114–122, 2015.

[24] H. Ak, M. Iphar, M. Yavuz, and A. Konuk, "Evaluation of ground vibration effect of blasting operations in a magnesite mine," *Soil Dynamics and Earthquake Engineering*, vol. 29, no. 4, pp. 669–676, 2009.

[25] K. Liu, H. Hao, and X. Li, "Numerical analysis of the stability of abandoned cavities in bench blasting," *International Journal of Rock Mechanics and Mining Sciences*, vol. 92, pp. 30–39, 2017.

[26] R. Yang, W. F. Bawden, and P. D. Katsabanis, "A new constitutive model for blast damage," *International Journal of Rock Mechanics and Mining Sciences & Geomechanics*, vol. 33, no. 3, pp. 245–254, 1996.

[27] M. Khandelwal and T. N. Singh, "Prediction of blast-induced ground vibration using artificial neural network," *International Journal of Rock Mechanics and Mining Sciences*, vol. 46, no. 7, pp. 1214–1222, 2009.

[28] M. Monjezi and H. Dehghani, "Evaluation of effect of blasting pattern parameters on back break using neural networks," *International Journal of Rock Mechanics and Mining Sciences*, vol. 45, no. 8, pp. 1446–1453, 2008.

[29] T. Lu, Y. Q. Shi, C. Huang et al., "Study on attenuation parameters of blasting vibration by nonlinear regression analysis," *Rock and Soil Mechanics*, no. 9, pp. 1871–1878, 2007.

[30] J. H. Hu, J. L. Shang, X. W. Luo et al., "Monitoring of single-hole blasting vibration and detection of its attenuation law by using multiple linear regression," *Journal of Vibration and Shock*, no. 16, pp. 49–53, 2013.

[31] M. Hasanipanah, H. Bakhshandeh Amnieh, H. Khamesi, D. Jahed Armaghani, S. Bagheri Golzar, and A. Shahnazar, "Prediction of an environmental issue of mine blasting: an imperialistic competitive algorithm-based fuzzy system," *International Journal of Environmental Science and Technology*, vol. 15, no. 3, pp. 551–560, 2016.

[32] N. Fouladgar, M. Hasanipanah, and H. B. Amnieh, "Application of cuckoo search algorithm to estimate peak particle velocity in mine blasting," *Engineering with Computers*, vol. 33, no. 2, pp. 181–189, 2017.

[33] M. Amiri, H. Bakhshandeh Amnieh, M. Hasanipanah, and L. Mohammad Khanli, "A new combination of artificial neural network and K-nearest neighbors models to predict blast-induced ground vibration and air-overpressure," *Engineering with Computers*, vol. 32, no. 4, pp. 631–644, 2016.

[34] M. Monjezi, M. Hasanipanah, and M. Khandelwal, "Evaluation and prediction of blast-induced ground vibration at Shur River Dam, Iran, by artificial neural network," *Neural Computing and Applications*, vol. 22, no. 7-8, pp. 1637–1643, 2013.

[35] K. Taheri, M. Hasanipanah, S. B. Golzar, and M. Z. A. Majid, "A hybrid artificial bee colony algorithm-artificial neural network for forecasting the blast-produced ground vibration," *Engineering with Computers*, vol. 33, no. 3, pp. 689–700, 2016.

[36] Y. Wan, Y. Gao, and F. Zhang, "Stability analysis of three-dimensional slopes considering the earthquake force direction," *Mathematical Problems in Engineering*, vol. 2018, Article ID 2381370, 10 pages, 2018.